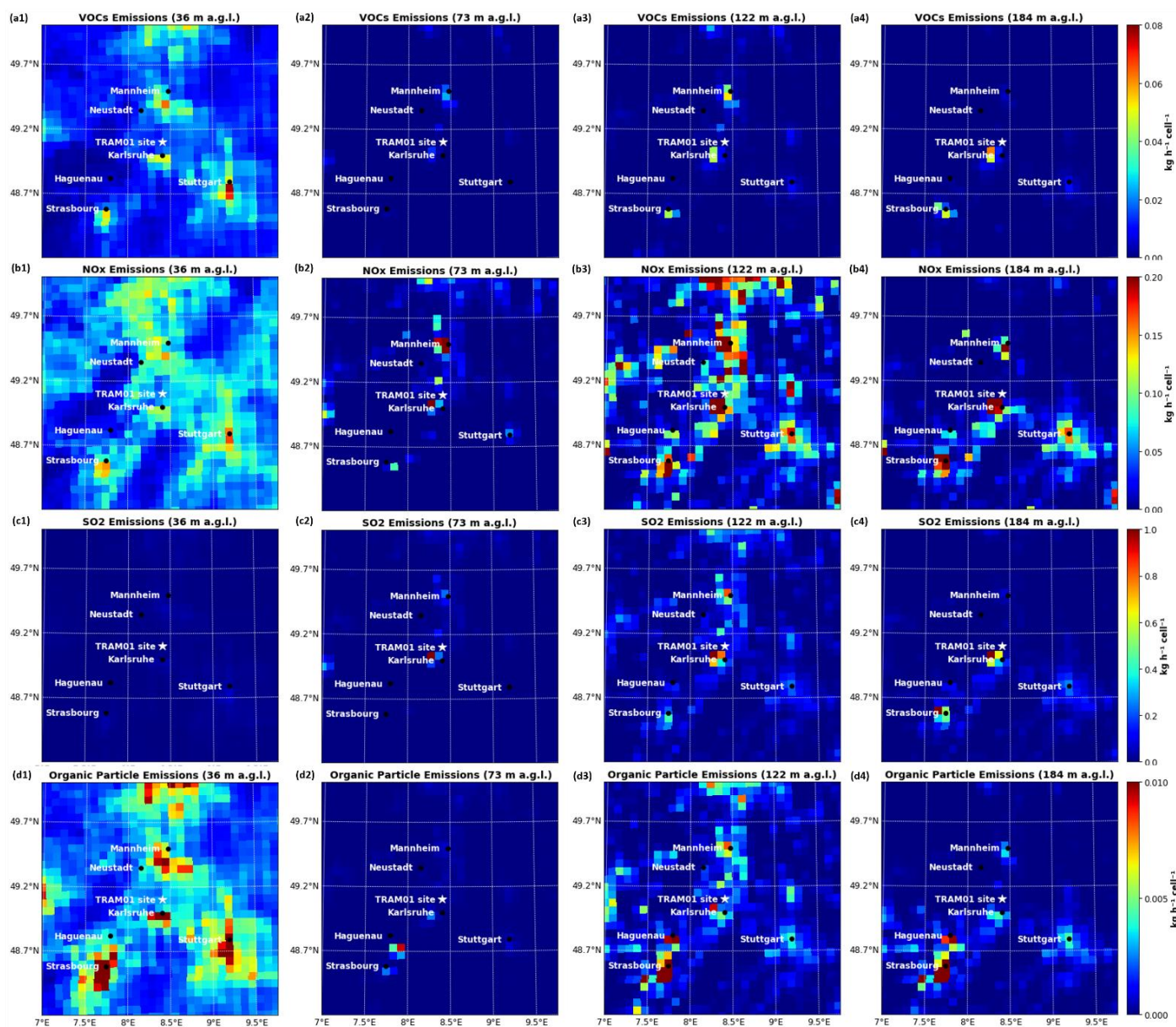


In order to study the nature and origin of aerosols at a rural site in the upper Rhine valley, we conducted a stationary measurement campaign (TRAM01) in summer 2016, and applied a transport model COSMO-ART to help source apportionment and to achieve a better understanding of the impact of complex transport pattern on the field observations. In the main manuscript, we have mainly discussed two selected episodes, one is rich in sodium chloride and another is rich in organics. Here is the supporting information, including figures, as well as some detailed descriptions.

5



10 **Figure S1: Emission maps of VOCs (a1 to a4), NOx (b1 to b4), SO₂ (c1 to c4), and primary organic particles (d1 to d4) at different altitudes, i.e., 36, 74, 122, and 184 m (from left to right) above ground level (a.g.l.).**

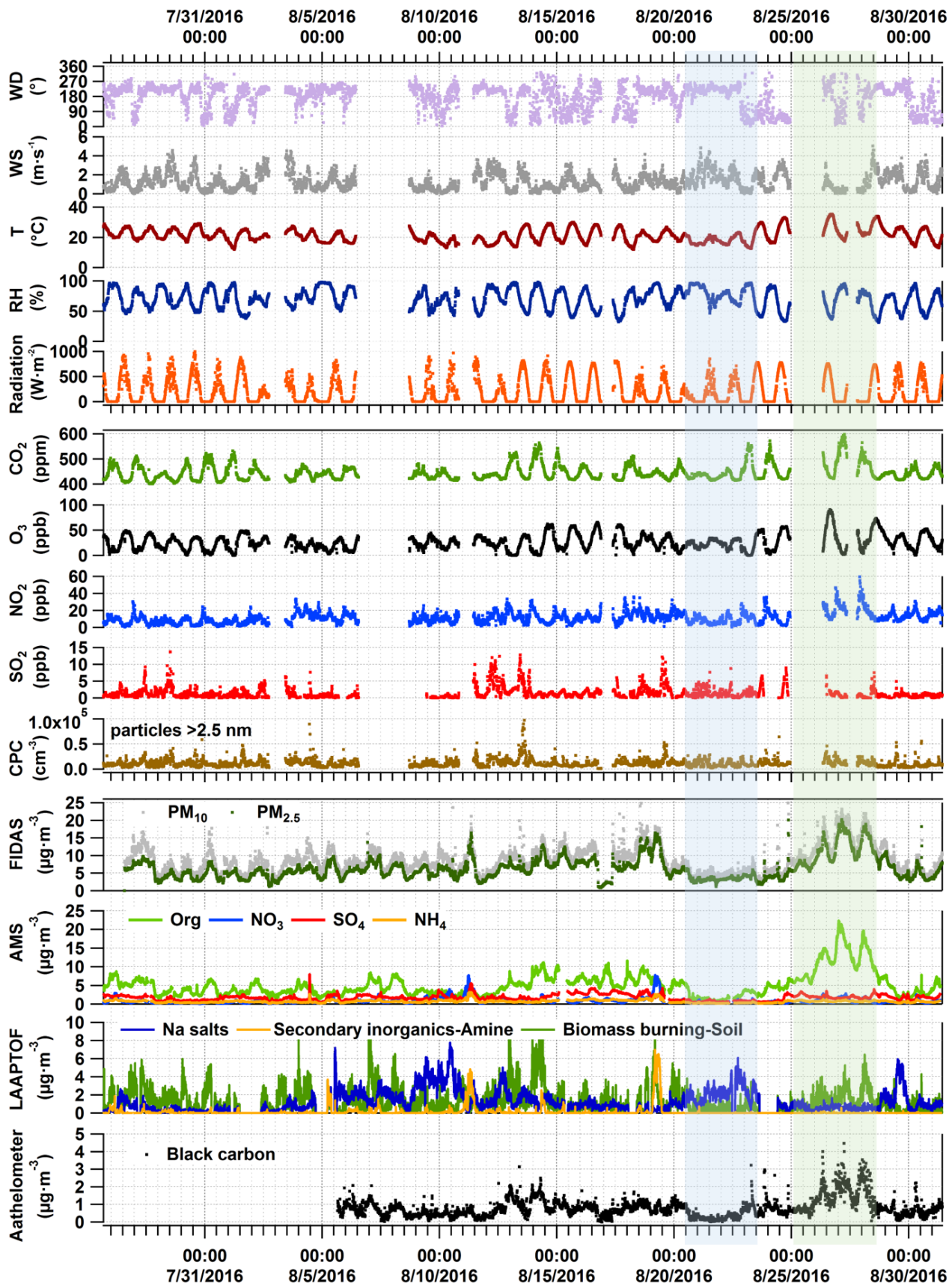
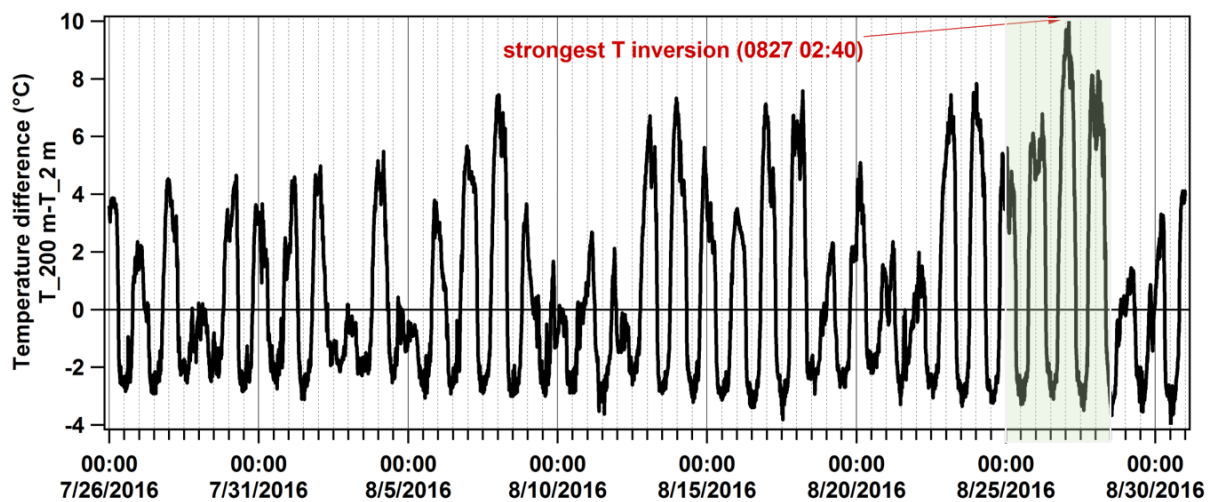


Figure S2: Overview of the whole measurement campaign including meteorology parameters, trace gases, and aerosol particle mass and composition. The first (blue) and second (green) shaded areas mark the sodium chloride rich and the organic rich episodes, respectively.



5 **Figure S3:** Time series of temperature difference between 200 m and 2 m above ground level (a.g.l.), measured at the KIT-tower. The bigger difference denotes the stronger temperature inversion. Temperature inversions are stronger during the organics rich episode marked with a shaded background. The strongest temperature inversion was measured at 02:40 on August 27.

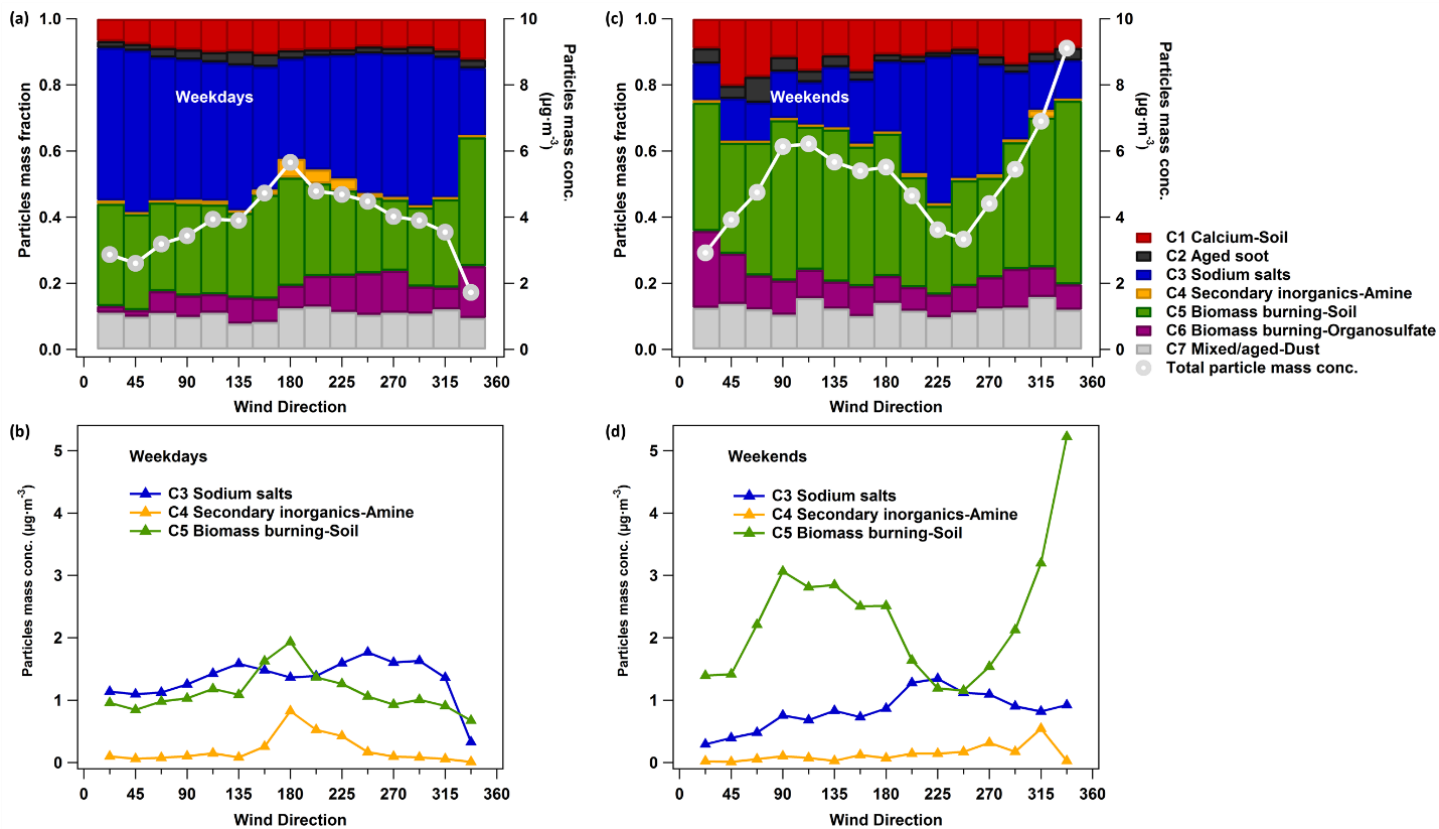


Figure S4: Comparison of particle classes measured by LAAPTOF as a function of wind direction for weekdays (left) and weekends (right).

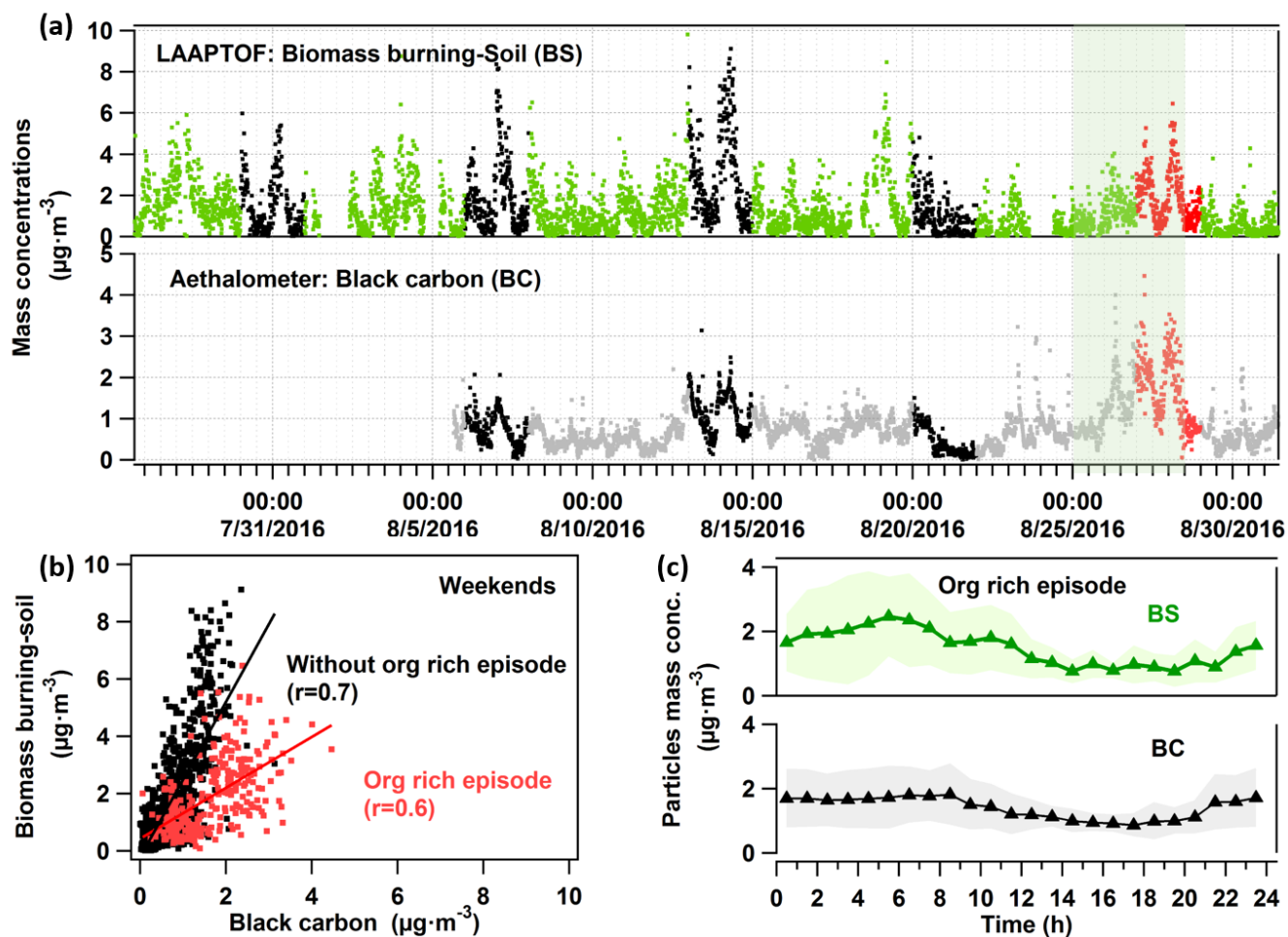


Figure S5: (a) Time series of aged-biomass-burning and soil-dust like particles and black carbon (black and red dots are weekend data); red dots are in organics rich episode. The shaded area marks the organics rich episode. (b) Comparison of mass concentration between biomass burning-soil and black carbon measured during the weekends. Black and red dots are the data without and with organic rich episode, respectively. (c) Diurnal pattern of particle mass concentration of biomass burning-soil (BS) and black carbon (BC) during organics rich episode, respectively.

5

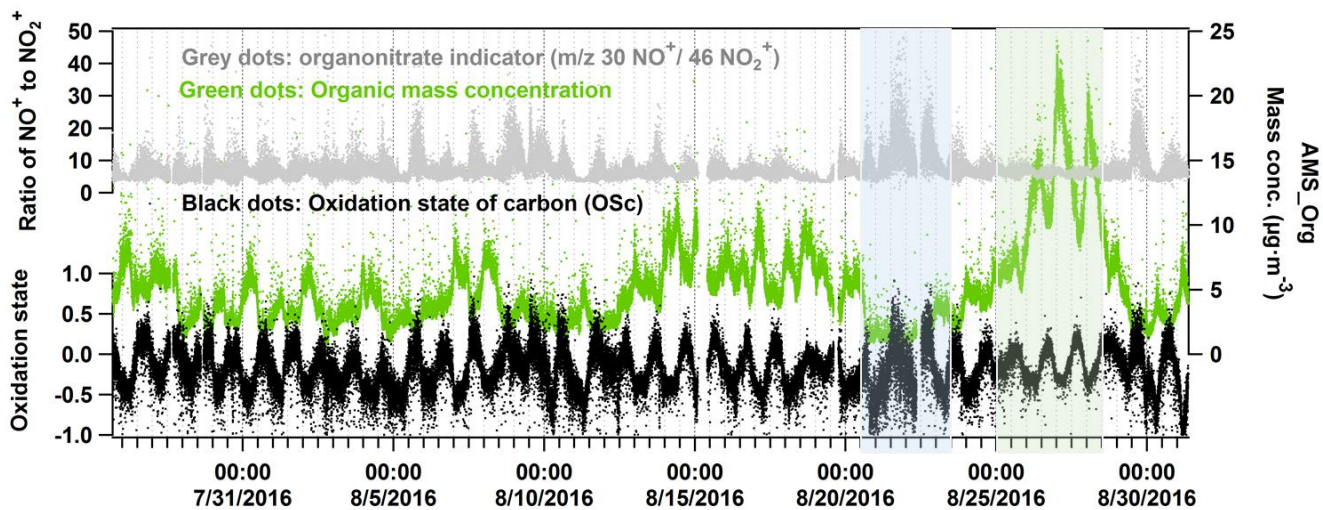


Figure S6: Time series of organonitrate indicator (grey dots) and oxidation state (black dots). The first (blue) and second (green) shaded areas mark the sodium chloride rich and organic rich episodes, respectively.

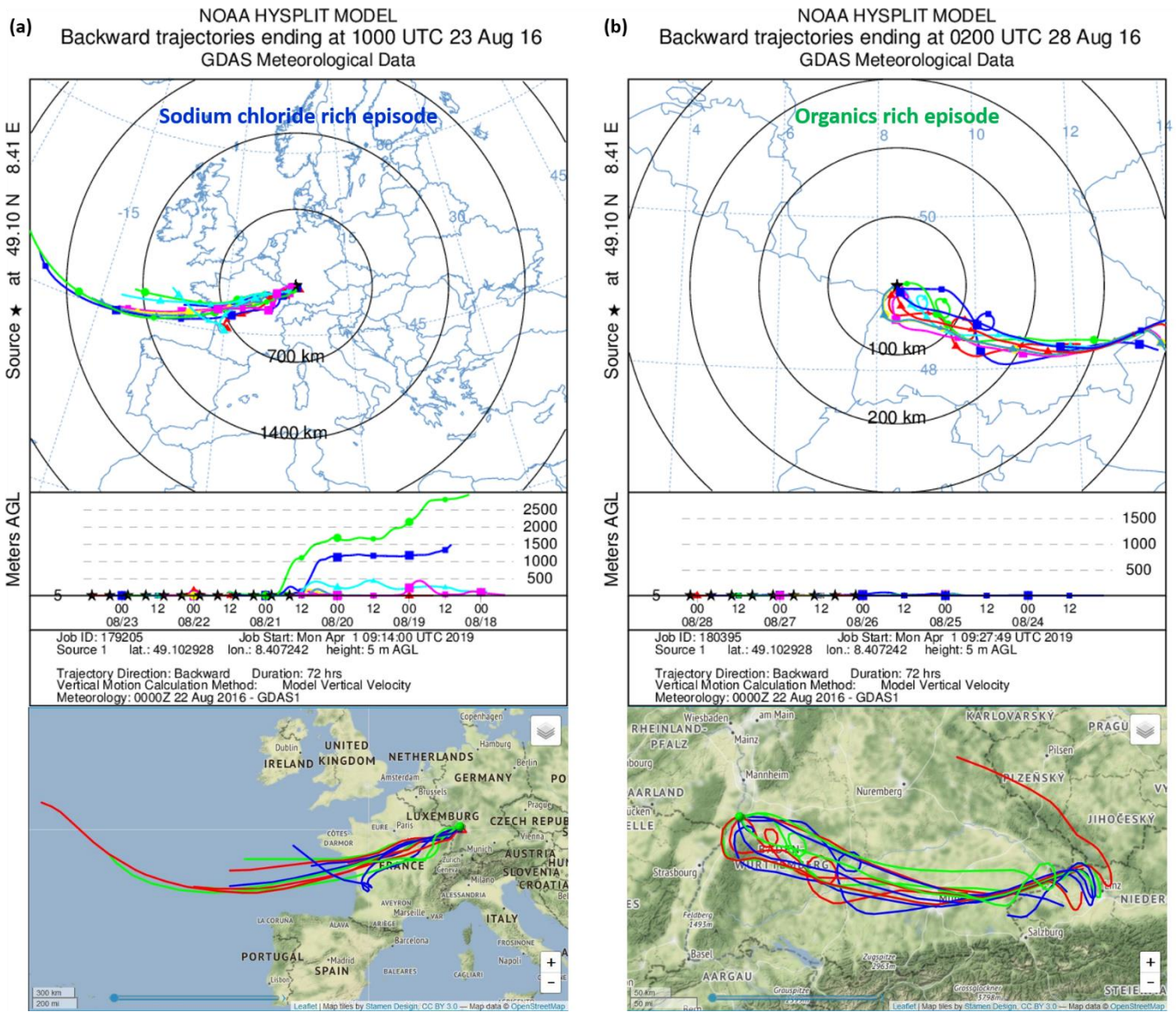


Figure S7: Hybrid Single-Particle Lagrangian Integrated Trajectory (HYSPLIT) back-trajectory analysis for 72 hours for sodium chloride rich (a) and organics rich (b) episodes, respectively.

5

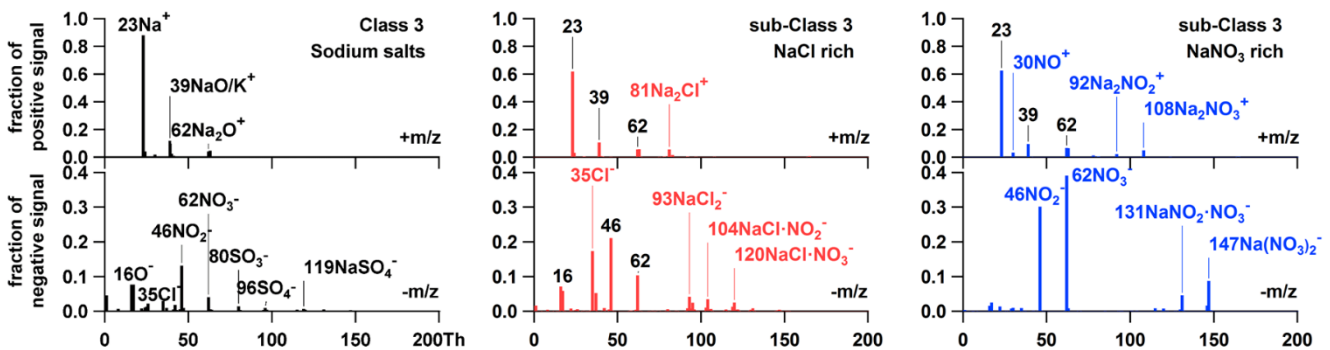
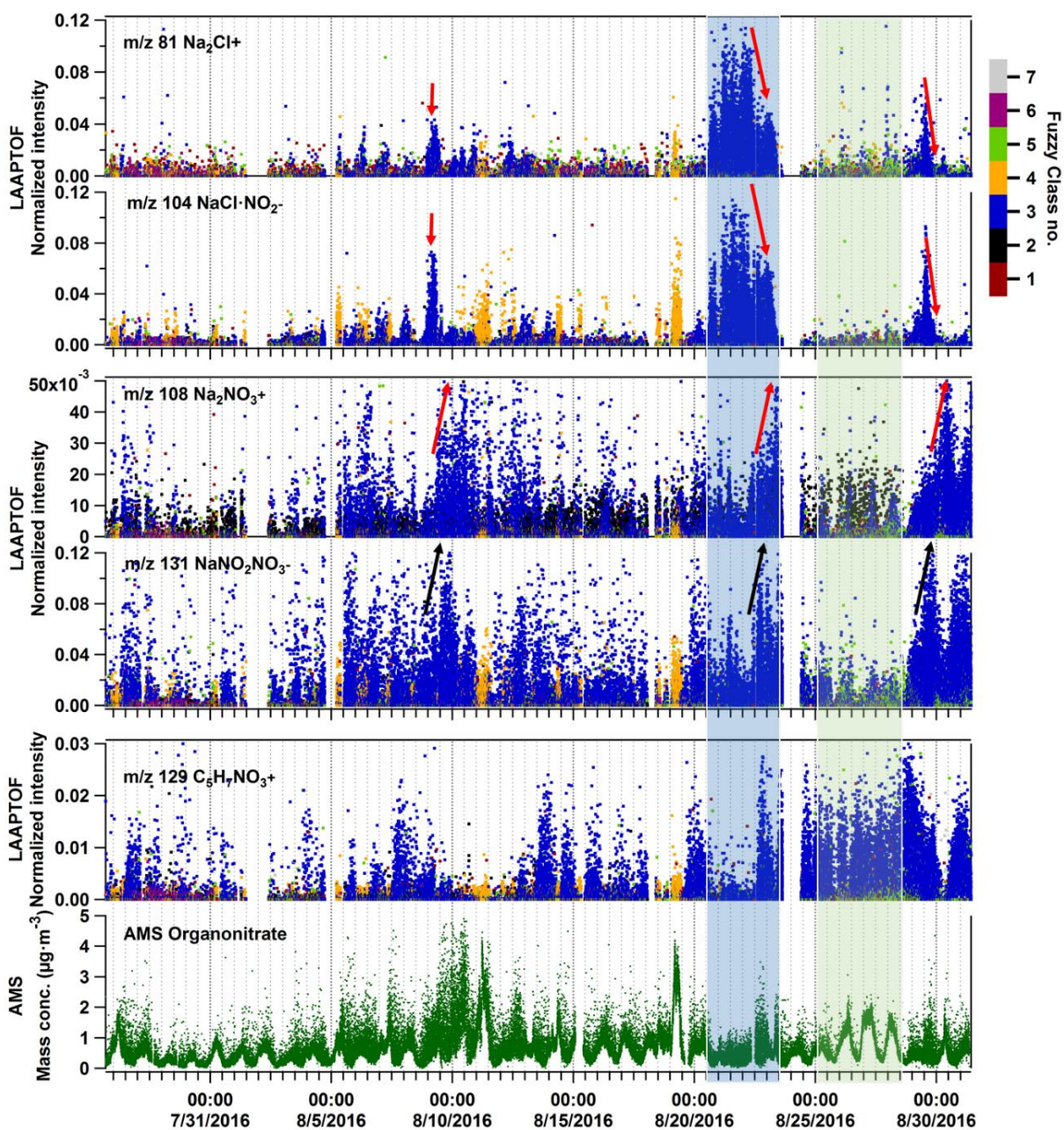


Figure S8: Spectra of the sodium salts class (Shen et al., 2019) and its sub-classes: NaCl rich (averaged from 1487 particles) and NaNO₃ rich (averaged from 300 particles).



5 Figure S9: Time series of sodium chloride, nitrate, and organonitrate. Y-axis is the normalized ion intensity (each ion peak intensity is normalized to the sum of all ion signals; positive and negative ions were analysed separately). The seven classes are class 1: calcium-Soil; class 2: aged soot; class3: sodium salts; class 4: secondary inorganics-amine; class 5: biomass burning-soil; class 6: biomass burning-organosulfate; and class 7: mixed/aged-dust. Obvious sodium chloride and nitrate signatures are mainly found in class 3 labelled in blue colour. The first (blue) and second (green) bands mark the sodium chloride rich and organic rich episodes, respectively.

10 The method to estimate organonitrate based on AMS measurement can be referred to Farmer et al. (2010) and the parameters used here are the same as that used by Huang et al. (2019). The result in Fig. S8 is based on our AMS measurements and the corresponding equation suggested by Farmer et al. (2010), as follows:

$$y = \frac{[(\text{Robs}-\text{Ran})(1+\text{Ron})]}{[(\text{Ron}-\text{Ran})(1+\text{Robs})]}$$
 where y is the estimated organonitrate mass concentration ($\mu\text{g m}^{-3}$), Robs is the observed ambient ratio of $\text{NO}_2^+/\text{NO}^+$; Ran and Ron are the $\text{NO}_2^+/\text{NO}^+$ ratio for ammonium nitrate and organonitrate, respectively. In our study $\text{Ran}=0.43$ based on the measurement and $\text{Ron}=0.1$ based on literature data. More details can be found by Huang et al. (2019).

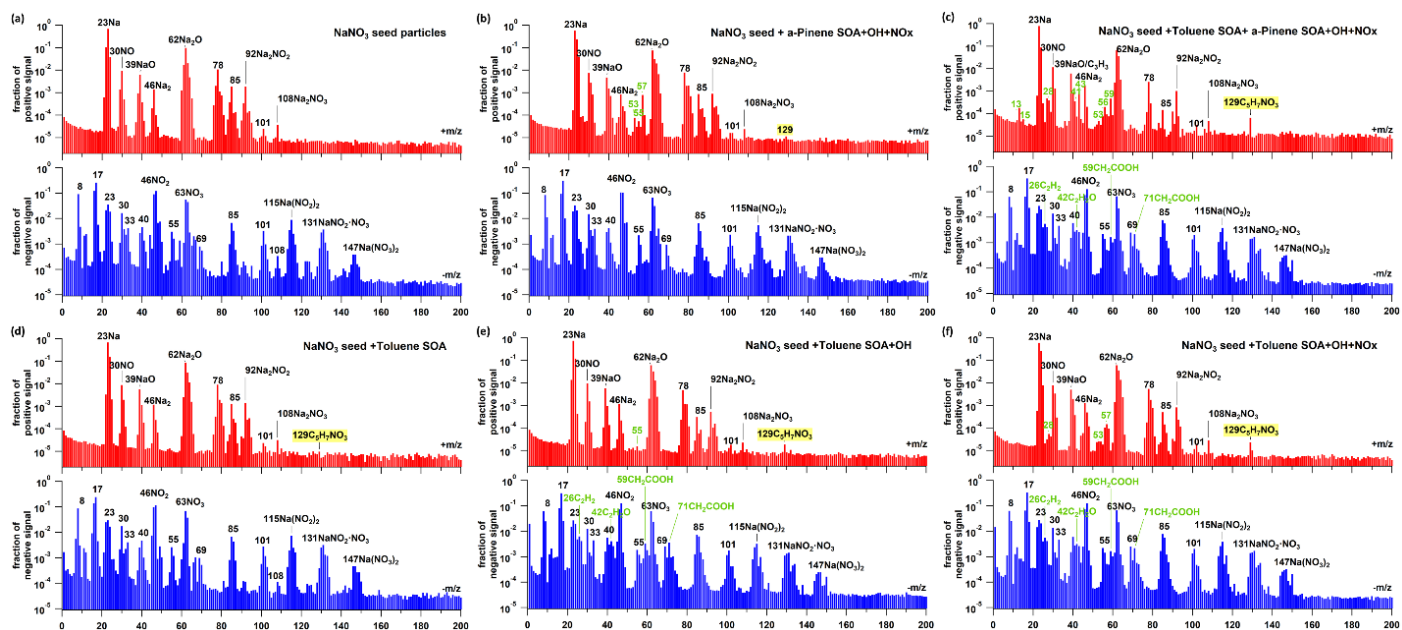


Figure S10: Laboratory evidence for anthropogenic organonitrate (LAAPTOF signature m/z 129 $C_5H_7NO_3^+$). (a) to (f) are the averaged spectra from several thousand single particles, respectively. Y-axis is the normalized ion intensity (each ion peak intensity is normalized to the sum of all ion signals; positive and negative ions were analysed separately).

5 Regarding organonitrate, we have found some laboratory evidence for its potential origin. AIDA (aerosol interaction and dynamics in the atmosphere) simulation chamber studies have been done with α -pinene and/or toluene OH oxidations on $NaNO_3$ seeds in the presence/absence of NO_x . The corresponding single particle mass spectra are shown in Fig. S9. It turns out that m/z 129+ is quite weak in α -pinene system even with NO_x (panel b), but it is much stronger after toluene is added (panel c). In the toluene system (refer to panel d to f), m/z 129+ is already present when $NaNO_3$ seeds are coated with toluene derived secondary organic aerosol (SOA) (panel d), likely due to the recombined fragments from toluene and nitrate. After adding extra OH, m/z 129+ is becoming stronger, likely due to the more aged toluene SOA. When NO_x is added to toluene system, m/z 129+ becomes much stronger (panel e), likely due to the organonitrate formation. Hence, we can conclude that m/z 129 $C_5H_7NO_3^+$ is more related to toluene rather than α -pinene, namely m/z 129 $C_5H_7NO_3^+$ could be a signature peak for anthropogenic sources in LAAPTOF spectra.

10

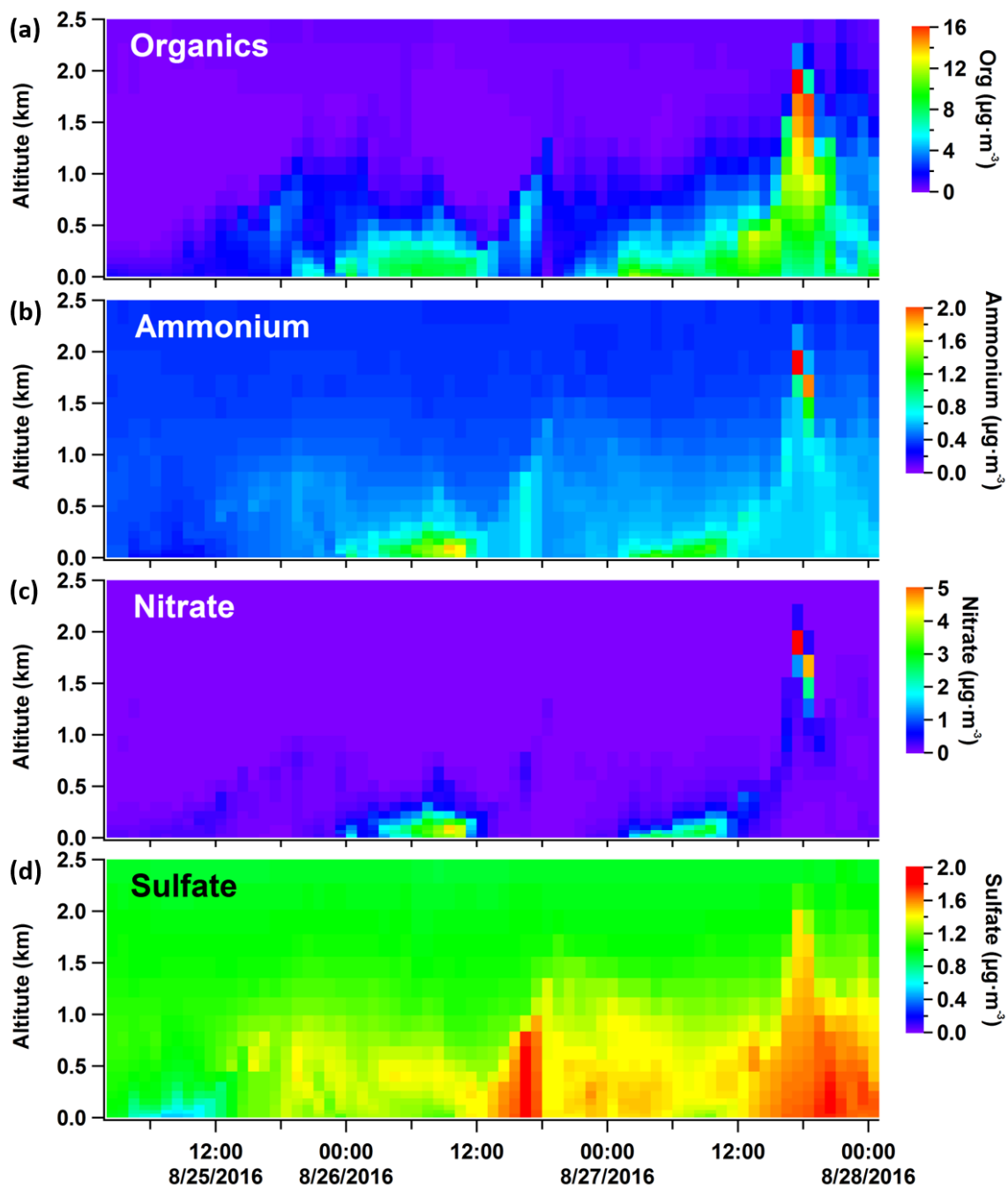


Figure S11: Time series of vertical profiles for organics, ammonium, nitrate, and sulfate as calculated by COSMO-ART.

References

- Farmer, D. K., Matsunaga, A., Docherty, K. S., Surratt, J. D., Seinfeld, J. H., Ziemann, P. J., and Jimenez, J. L.: Response of an aerosol mass spectrometer to organonitrates and organosulfates and implications for atmospheric chemistry, *P Natl Acad Sci USA*, 107, 6670–6675, 2010.
- 5 Huang, W., Saathoff, H., Shen, X. L., Ramakrishna, R., Leisner, T., and Mohr, C.: Chemical characterization of highly functionalized organonitrates contributing to high night-time organic aerosol mass loadings and particle growth, *Environ Sci Technol*, 53, 1165–1174, 2019.
- 10 **Five supporting videos (.gif files) are available at KIT open data (<https://doi.org/10.5445/IR/1000094401>).**
- 1. SI_PN_10m.gif**
- Particle number concentrations and wind field calculated by COSMO-ART during high SO₂ period (from 20160826 0:00 to 13:00 (local time) for 10 m a.g.l.
- 2. SI_PN_122m.gif**
- 15 Particle number concentrations and wind field calculated by COSMO-ART during high SO₂ period from 20160826 0:00 to 13:00 (local time) for 122 m a.g.l.
- 3. SI_Org1_10m.gif**
- Particulate organic mass concentrations and wind field calculated by COSMO-ART from 20160825 17:00 to 20160826 18:00 (local time) for 10 m a.g.l.
- 20 **4. SI_Org2_10m.gif**
- Particulate organic mass concentrations and wind field calculated by COSMO-ART from 20160826 18:00 to 20160827 12:00 (local time) for 10 m a.g.l.
- 5. SI_Org3_10m.gif**
- 25 Particulate organic mass concentrations and wind field calculated by COSMO-ART from 20160827 12:00 to 20160828 01:00 (local time) for 10 m a.g.l.